A Search for Single Photon Events in Neutrino Interactions in NOMAD

C.T. Kullenberg [s] S.R. Mishra [s] D. Dimmery [s] X.C. Tian [s]
D. Autiero [h] S. Gninenko [h,ℓ] A. Rubbia [h,x] S. Alekhin [y]
P. Astier [n] A. Baldisseri [r] M. Baldo-Ceolin [m] M. Banner [n]
G. Bassompierre [a] K. Benslama [i] N. Besson [r] I. Bird [h,i]
B. Blumenfeld [b] F. Bobisut [m] J. Bouchez [r] S. Boyd [t,1]
A. Bueno [c,x] S. Bunyatov [f] L. Camilleri [h] A. Cardini [j]
P.W. Cattaneo [o] V. Cavasinni [p] A. Cervera-Villanueva [h,v]
R. Challis [k] A. Chukanov [f] G. Collazuol [m] G. Conforto [h,u,2]
C. Conta [o] M. Contalbrigo [m] R. Cousins [j] H. Degaudenzi [i]
A. De Santo [h,p] T. Del Prete [p] L. Di Lella [h,3]
E. do Couto e Silva [h] J. Dumarchez [n] M. Ellis [t,4] G.J. Feldman [c]
R. Ferrari [o] D. Ferrère [h] V. Flaminio [p] M. Fraternali [o]
J.-M. Gaillard [a] E. Gangler [h,n] A. Geiser [e,h] D. Geppert [e]
D. Gibin [m] A. Godley [s] J.-J. Gomez-Cadenas [h,v] J. Gosset [r]
C. Gößling [e] M. Gouanère [a] A. Grant [h] G. Graziani [g]
A. Guglielmi [m] C. Hagner [r] J. Hernando [v] P. Hurst [c] N. Hyett [k]
E. Iacopini [g] C. Joseph [i] F. Juget [i] N. Kent [k] O. Klimov [f]
J. Kokkonen [h] A. Kovzelev [ℓ,o] A. Krasnoperov [a,f] J.J. Kim [s]
M. Kirsanov [ℓ] S. Kulagin [ℓ] S. Lacaprara [m] C. Lachaud [n]
B. Lakić [w] A. Lanza [o] L. La Rotonda [d] M. Laveder [m]
A. Letessier-Selvon [n] J.-M. Levy [n] J. Ling [s] L. Linssen [h]
A. Ljubičić [w] J. Long [b] A. Lupi [g] V. Lyubushkin [f]
A. Marchionni [g] F. Martelli [u] X. Méchain [r] J.-P. Mendiburu [a]
J.-P. Meyer [r] M. Mezzetto [m] G.F. Moorhead [k] D. Naumov [f]
P. Nédélec [a] Yu. Nefedov [f] C. Nguyen-Mau [i] D. Orestano [q]
F. Pastore [q] L.S. Peak [t] E. Pennacchio [u] H. Pessard [a] R. Petti [s]
A. Placci [h] G. Polesello [o] D. Pollmann [e] A. Polyarush [ℓ]
C. Poulsen [k] B. Popov [f,n] L. Rebuffi [m] J. Rico [x] P. Riemann [e]
C. Roda [h,p] F. Salvatore [o] O. Samoylov [f] K. Schahmaneche [n]
B. Schmidt [e,h] T. Schmidt [e] A. Sconza [m] A.M. Scott [s]

Preprint submitted to Physics Letters B *17 November 2011*

M.B. Seaton [s] M. Sevior [k] D. Sillou [a] F.J.P. Soler [h,t] G. Sozzi [i]
D. Steele [b,i] U. Stiegler [h] M. Stipčević [w] Th. Stolarczyk [r]
M. Tareb-Reyes [i] G.N. Taylor [k] V. Tereshchenko [f] A. Toropin [ℓ]
A.-M. Touchard [n] S.N. Tovey [h,k] M.-T. Tran [i] E. Tsesmelis [h]
J. Ulrichs [t] L. Vacavant [i] M. Valdata-Nappi [d,5] V. Valuev [f,j]
F. Vannucci [n] K.E. Varvell [t] M. Veltri [u] V. Vercesi [o]
G. Vidal-Sitjes [h] J.-M. Vieira [i] T. Vinogradova [j] F.V. Weber [c,h]
T. Weisse [e] F.F. Wilson [h] L.J. Winton [k] Q. Wu [s,6] B.D. Yabsley [t]
H. Zaccone [r] K. Zuber [e] P. Zuccon [m]

[a] *LAPP, Annecy, France*
[b] *Johns Hopkins Univ., Baltimore, MD, USA*
[c] *Harvard Univ., Cambridge, MA, USA*
[d] *Univ. of Calabria and INFN, Cosenza, Italy*
[e] *Dortmund Univ., Dortmund, Germany*
[f] *JINR, Dubna, Russia*
[g] *Univ. of Florence and INFN, Florence, Italy*
[h] *CERN, Geneva, Switzerland*
[i] *University of Lausanne, Lausanne, Switzerland*
[j] *UCLA, Los Angeles, CA, USA*
[k] *University of Melbourne, Melbourne, Australia*
[ℓ] *Inst. for Nuclear Research, INR Moscow, Russia*
[m] *Univ. of Padova and INFN, Padova, Italy*
[n] *LPNHE, Univ. of Paris VI and VII, Paris, France*
[o] *Univ. of Pavia and INFN, Pavia, Italy*
[p] *Univ. of Pisa and INFN, Pisa, Italy*
[q] *Roma Tre University and INFN, Rome, Italy*
[r] *DAPNIA, CEA Saclay, France*
[s] *Univ. of South Carolina, Columbia, SC, USA*
[t] *Univ. of Sydney, Sydney, Australia*
[u] *Univ. of Urbino, Urbino, and INFN Florence, Italy*
[v] *IFIC, Valencia, Spain*
[w] *Rudjer Bošković Institute, Zagreb, Croatia*
[x] *ETH Zürich, Zürich, Switzerland*
[y] *Inst. for High Energy Physics, 142281, Protvino, Moscow, Russia*

Abstract

We present a search for neutrino-induced events containing a single, exclusive photon using data from the NOMAD experiment at the CERN SPS where the average energy of the neutrino flux is $\simeq$ 25 GeV. The search is motivated by an excess of electron-like events in the 200–475 MeV energy region as reported by the MiniBOONE experiment. In NOMAD, photons are identified via their conversion to e^+e^- in an active target embedded in a magnetic field. The background to the single photon signal is dominated by the asymmetric decay of neutral pions produced either in a coherent neutrino-nucleus interaction, or in a neutrino-nucleon neutral current deep inelastic scattering, or in an interaction occurring outside the fiducial volume. All three backgrounds are determined *in situ* using control data samples prior to opening the 'signal-box'. In the signal region, we observe **155** events with a predicted background of $\mathbf{129.2 \pm 8.5 \pm 3.3}$. We interpret this as null evidence for excess of single photon events, and set a limit. Assuming that the hypothetical single photon has a momentum distribution similar to that of a photon from the coherent π^0 decay, the measurement yields an upper limit on single photon events, $\mathbf{< 4.0 \times 10^{-4}}$ per $\boldsymbol{\nu_\mu}$ charged current event. Narrowing the search to events where the photon is approximately collinear with the incident neutrino, we observe **78** events with a predicted background of $\mathbf{76.6 \pm 4.9 \pm 1.9}$ yielding a more stringent upper limit, $\mathbf{< 1.6 \times 10^{-4}}$ per $\boldsymbol{\nu_\mu}$ charged current event.

Key words: single-photon neutrino neutral current coherent pion
PACS: 13.15.+g, 13.85.Lg, 14.60.Lm

1 The Question

The MiniBooNE experiment, in the neutrino-mode, has reported an excess of 129±43 (Stat ⊕Syst) electron-like events in the 200–475 MeV energy range [1], a range largely unaffected by the $\boldsymbol{\nu_\mu \to \nu_e}$ oscillations at $\Delta m^2 > 1$ eV^2, which is expected to dominate the 475-1250 MeV range [2]. Assuming that the efficiency of these events is 0.25, similar to that of the $\boldsymbol{\nu_e}$-induced electrons, the rate of the excess with respect to $\boldsymbol{\nu_\mu}$-CC is $\simeq 3 \times 10^{-3}$. In the antineutrino mode, initially the MiniBOONE data were consistent with background in the 200–475 MeV range [3]. Recently, with additional antineutrino data, they

[1] Now at University of Warwick, UK
[2] Deceased
[3] Now at Scuola Normale Superiore, Pisa, Italy
[4] Now at Brunel University, Australia
[5] Now at Univ. of Perugia and INFN, Perugia, Italy
[6] Now at Illinois Institute of Technology, USA

report a 2σ excess in this region [4]. MiniBOONE lacks the resolution to determine if the excess is due to e^-, e^+, or a photon. In neutrino interactions single photons do not occur: they occur in pairs from the $\pi^0 \to \gamma\gamma$ decay. Evidence of events with a single photon and nothing else in neutrino induced neutral current (NC) interaction will signal either new or unconventional physics. This anomaly needs to be checked experimentally.

The low-energy MiniBOONE excess has motivated novel hypotheses invoking conventional, to unconventional, to entirely new physics processes. An explanation [5] of the excess attributed to the internal bremsstrahlung associated with muons in $\boldsymbol{\nu_\mu}$-induced charged current interaction (CC) has been refuted by MiniBooNE [6]. Harvey, Hill, and Hill [7,8] postulate a new anomaly-mediated interaction between the ν-induced Z^0-boson, the photon, and a vector meson, such as ω, coupling strongly to the target nucleus. A similar, single photon process has been envisioned by Jenkins & Goldman [9]. In the anomaly-mediated neutrino-photon (ANP) interaction, $\nu\mathcal{N} \to \nu\mathcal{N}\gamma$, where $\mathcal{N}$ is the target nucleus or nucleon, the observable is a single $\boldsymbol{\gamma}$, approximately collinear with the incident neutrino direction in the lab frame with a recoiling $\boldsymbol{\mathcal{N}}$ which remains intact and largely undetected; the form factor of $\boldsymbol{\mathcal{N}}$ is expected to induce the single $\boldsymbol{\gamma}$ to be pulled forward. The ANP cross-section is expected to increase with neutrino energy ($\boldsymbol{E_\nu}$). The ANP interaction is akin to the exclusive $\boldsymbol{\pi^0}$ production when the neutrino coherently scatters off a target nucleus (Coh$\boldsymbol{\pi^0}$), $\boldsymbol{\nu + \mathcal{N} \to \nu + \mathcal{N} + \pi^0}$, where the only observable is $\boldsymbol{\pi^0 \to \gamma\gamma}$. The phenomenology of ANP developed by Hill in [10], and largely focussed on the low energy neutrino interaction ($\boldsymbol{E_\nu \simeq \mathcal{O}(1)}$ GeV), predicts a cross-section sufficiently large to explain the MiniBOONE anomaly. If true, the ANP interaction will also impact astrophysical processes such as neutron star cooling. Hypotheses involving new physics include: decay of a heavy neutrino into a light neutrino and a photon, $\boldsymbol{\nu_h \to \nu + \gamma}$, by Gninenko [11,12]; CP-violation in 3$\oplus$ 2 model by Maltoni & Schwetz [13], and by Goldman *et al.* [14]; extra-dimensions in 3$\oplus$1 model by Pas *et al.* [15]; and models by Giunti and Laveder [16]; Lorentz-violation by Katori *et al.* [17]; CPT-violation in 3$\oplus$1 model by Barger *et al.* [18]; new gauge bosons with sterile neutrinos by Nelson & Walsh [19]; and soft-decoherence by Farzan *et al.* [20]; etc. The NOMAD collaboration has reported a search of heavy-$\boldsymbol{\nu}$ which mixes with $\boldsymbol{\nu_\tau}$'s produced in the SPS proton-target, and then decays into $\boldsymbol{e^-e^+}$ pair in the detector [21]. The search focussed on highly collinear ($\boldsymbol{\mathcal{C} = [1 - cos\Theta_{ee}] \leq 2 \times 10^{-5}}$) and high energy ($\boldsymbol{E_{ee} \geq 4}$ GeV) $\boldsymbol{e^-e^+}$ events, where $\boldsymbol{\Theta_{ee}}$ and $\boldsymbol{E_{ee}}$ are the polar angle and the energy of the converted photon, and resulted in a single event consistent with the estimated background. The present work extends this search with no cut on $\boldsymbol{\mathcal{C}}$.

The high resolution NOMAD data allow a sensitive search for neutrino induced single photon events ($1\boldsymbol{\gamma}$). The detector measures the energy and emission angle of the photon. Additionally, the detector affords the redundancy to

measure *in situ* all relevant backgrounds relieving the reliance on Monte Carlo simulation (MC) of the conventional processes. As regards the MiniBooNE low-energy anomaly, we note that the average energy of the SPS neutrino flux at NOMAD, $\boldsymbol{E_\nu \simeq 25}$ GeV, is much higher than that of MiniBOONE, $\boldsymbol{E_\nu \simeq 1}$ GeV. However, the NOMAD data provide a stringent check in a different energy range. If a mechanism explaining the anomaly were applicable to higher energies, such as ANP or $\boldsymbol{\nu}$-decay hypotheses, then this search, even if negative, will furnish meaningful limits.

2 Beam and Detector

The Neutrino Oscillation MAgnetic Detector (NOMAD) experiment at CERN used a neutrino beam produced by the 450 GeV protons from the Super Proton Synchrotron (SPS) incident on a beryllium target and producing secondary $\boldsymbol{\pi^\pm}$, $\boldsymbol{K^\pm}$, and $\boldsymbol{K^0}$ mesons. The positively charged mesons were focussed by two magnetic horns into a 290 m long evacuated decay pipe. Decays of $\boldsymbol{\pi^\pm}$, $\boldsymbol{K^\pm}$, and $\boldsymbol{K^0_L}$ produced the SPS neutrino beam. The average neutrino flight path to NOMAD was 628 m, the detector being 836 m downstream of the Be-target. The SPS beamline and the neutrino flux incident at NOMAD are described in [22]. The $\boldsymbol{\nu}$-flux in NOMAD is constrained by the $\boldsymbol{\pi^\pm}$ and $\boldsymbol{K^\pm}$ production measurements in proton-Be collision by the SPY experiment [23,24,25] and by an earlier measurement conducted by Atherton *et al.* [26]. The $\boldsymbol{E_\nu}$-integrated relative composition of $\boldsymbol{\nu_\mu}$:$\boldsymbol{\overline{\nu}_\mu}$:$\boldsymbol{\nu_e}$:$\boldsymbol{\overline{\nu}_e}$ CC events, constrained *in situ* by the measurement of CC-interactions of each of the neutrino species, is **1.00 : 0.025 : 0.015 : 0.0015**. Thus, 97.5% of the events are induced by neutrinos with a small anti-neutrino contamination, similar to that reported by MiniBOONE [2].

The NOMAD apparatus, described in [27], was composed of several subdetectors. The active target comprised 132 planes of $\boldsymbol{3 \times 3}$ m$^{\boldsymbol{2}}$ drift chambers (DC) with an average density similar to that of liquid hydrogen (0.1 gm/cm$^{\boldsymbol{3}}$). On average, the equivalent material in the DC encountered by particles produced in a $\boldsymbol{\nu}$-interaction was about half of a radiation length and a quarter of a hadronic interaction length ($\boldsymbol{\lambda}$). The fiducial mass of the NOMAD DC-target, 2.7 tons, was composed primarily of carbon (64%), oxygen (22%), nitrogen (6%), and hydrogen (5%) yielding an effective atomic number, $\boldsymbol{\mathcal{A}}$ =12.8, similar to carbon. Downstream of the DC, there were nine modules of transition radiation detectors (TRD), followed by a preshower (PRS) and a lead-glass electromagnetic calorimeter (ECAL). The ensemble of DC, TRD, and PRS/ECAL was placed within a dipole magnet providing a 0.4 T magnetic field orthogonal to the neutrino beam line. Two planes of scintillation counters, $\boldsymbol{T_1}$ and $\boldsymbol{T_2}$, positioned upstream and downstream of the TRD, provided the trigger in combination with an anti-coincidence signal, $\boldsymbol{\overline{V}}$, from the veto counter up-

stream and outside the magnet. Downstream of the magnet was a hadron calorimeter, followed by two muon-stations each comprising large area drift chambers and separated by an iron filter. The two stations, placed at 8- and 13-$\boldsymbol{\lambda}$'s downstream of the ECAL, provided a clean identification of the muons. The schematic of the DC-tracker with a $\boldsymbol{\gamma}$-conversion in the Y-Z view is shown in Figure 1. The charged tracks in the DC were measured with an approximate momentum ($\boldsymbol{p}$) resolution of $\boldsymbol{\sigma_p/p = 0.05/\sqrt{L} \oplus 0.008p/\sqrt{L^5}}$ ($\boldsymbol{p}$ in GeV/$\boldsymbol{c}$ and $\boldsymbol{L}$ in meters) with unambiguous charge separation in the energy range of interest. The experiment recorded over 1.7 million neutrino interactions in the active drift-chamber (DC) target in the range $\boldsymbol{\mathcal{O}(1) \leq E_\nu \leq 300}$ GeV.

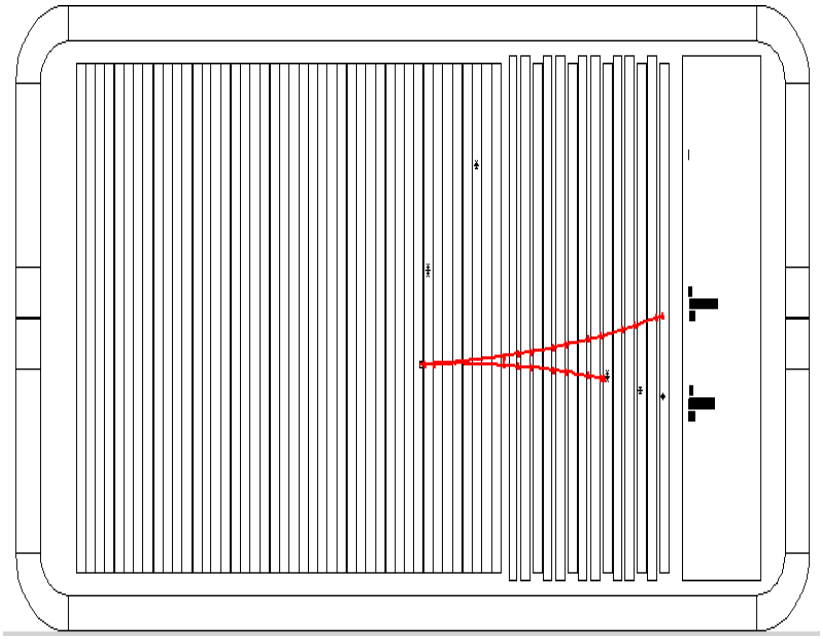

Fig. 1. Schematic of the DC tracker with a single γ-conversion event in NOMAD in Y (vertical) vs Z (horizontal) view. The energy and angle with respect to the neutrino direction of the γ are 3.1 GeV and 0.095 Radians.

3 The Exclusive Photon Signature

In NOMAD the cleanest signature of a γ is a $\mathbf{V^0}$ arising from its conversion in the DC into e^- and e^+ tracks as shown in Figure 1. The γ -momentum is reconstructed by measuring the 3-momenta of the associated e^-/e^+ tracks in the DC. The ECAL measures energy associated with the e^-/e^+ tracks plus any unconverted photons. Because the trigger counters are situated at the downstream end of the detector, only a fraction of events containing single photon will trigger the apparatus, namely events where the photon undergoes conversion in DC and the resulting e^+ or e^- traverses the trigger counters. Events with unconverted photons reaching the ECAL will not trigger the apparatus. For example, about 29% of the Coh$\boldsymbol{\pi^0}$ events, containing a $\boldsymbol{\pi^0}$ and 'nothing else', trigger the apparatus; the loss arises from the unconverted photons and, among the converted photons, from the e^-/e^+ tracks that do not reach the downstream trigger counters.

Single photon events will manifest as a $\mathbf{V^0}$, composed of e^- and e^+, with no additional energy in the ECAL. A converted photon is defined as a $\mathbf{V^0}$ such that the invariant mass of the e^- and e^+ (M_{ee}) is less than 100 MeV which selects the converted photons with 95% purity and 97% efficiency. Furthermore, if the single photon is approximately collinear with the incident neutrino then the collinearity of the photon-track offers an additional kinematic handle. Because we do not have a definitive simulation for the single

γ process, we use one of the photons from the Cohπ^0 , while ignoring the other photon, as a *guide* for the signal. We define two signal boxes. **Box1** comprises single γ events with negligible energy in the ECAL associated with neutral particles (γ , neutron, etc.) quantified by the quantity, $\mathbf{PAN} = [E_\gamma - E_{Neut}] \,/\, [E_\gamma + E_{Neut}] \geq 0.9$, where E_γ is the energy of the photon derived from the e^-/e^+ tracks and E_{Neut} is the ECAL energy associated with other neutral particles, i.e. not associated with e^+/e^- tracks. (For calculation of E_{Neut} see, for example, [28].) The $\mathbf{PAN} \geq 0.9$ cut is model independent. **Box2**, a subset of **Box1**, comprises single γ events provided that they are approximately collinear with the incident neutrino, characterized by the variable, $\zeta = E_\gamma \left[1 - \cos(\theta_\gamma)\right] \leq 0.05$, where E_γ and θ_γ are the photon's energy and polar angle with respect to the neutrino beam. (The variable ζ has the property that its distribution depends weakly on the incident neutrino energy.) Approximately 90% of the photons from Cohπ^0 have $\zeta \leq 0.05$. Although the $\zeta \leq 0.05$ cut will be somewhat model-dependent, at the SPS energies ($E_\nu \simeq 25$ GeV) most exotic models suggest that the single photon will be approximately collinear with the incident neutrino.

The backgrounds to the single γ are all interactions where all daughter particles, except one photon, evade detection. The background includes the Cohπ^0 interaction, the deep inelastic ν-NC scattering (NC-DIS), and ν-interactions occurring outside the fiducial volume (OBG). Note, that with a single converted γ in DC the coordinates of the ν-interaction cannot be ascertained. The sample with $\mathbf{PAN} < 0.9$ is composed of events with a $\mathbf{V^0}$ and neutral energy in the ECAL as expected from a π^0 decay and constitutes an important control sample. All three backgrounds are determined *in situ* as described below.

The analysis proceeds as follows. First, the sample with a single photon-conversion in DC is selected. Second, the three backgrounds to the single photon sample are calibrated using data outside **Box1**. The analysis leads to an experimentally constrained prediction of the background events in the signal region, **Box1** and **Box2**. Finally, boxes are opened and the predictions are compared with the observed data.

4 Selection of Single Photon Events

We select ν-induced events where a single photon converts ($\mathbf{V^0}$) within the fiducial volume of the DC target. The analysis uses the entire NOMAD data and the associated Monte Carlo (MC) samples described in [29]. The NC-DIS sample, defined by requiring that the generated invariant hadronic mass squared ($\mathbf{W^2}$) be ≥ 1.96 GeV^2, is normalized to 0.53×10^6 events which corresponds to 37% of the ν_μ-CC. The normalization of the NC-Resonance

Cut	Coh$\boldsymbol{\pi^0}$	NC-Res	NC-DIS MC	Data
Fiducial Cut	4,900	20,000	530,000	4,018,980
$\boldsymbol{\mu}$ID-veto & Single $\boldsymbol{\gamma}$-Induced $\mathbf{V^0}$	819	306	4,330	34,062
($\boldsymbol{M_{ee} \leq 100}$ MeV)				
$\mathbf{\lvert X, (Y-5)\rvert_{PROJ} \leq 130}$ cm	719	138	3,076	10,547
$\boldsymbol{E_{ee} \geq 1.5}$ GeV	516	69	1,846	4,543

Table 1
Preselection of events with a single, converted $\boldsymbol{\gamma}$ in Coh$\boldsymbol{\pi^0}$, NC-Resonance, and NC-DIS MC samples, and data. The MC samples, having a much larger statistics than data, are normalized to the expectation as described in the text. The $\mathbf{\lvert(X, Y-5)\rvert_{PROJ}}$ refer to X- and Y-position of the $\boldsymbol{\gamma}$-vector when projected to the most upstream DC ($\mathbf{Z_{Min}}$).

($\mathbf{W^2 < 1.96}$) sample is set at 3.5% of the NC-DIS. The Coh$\boldsymbol{\pi^0}$ interaction is simulated using the Rein-Sehgal (RS) model [30] which agrees well with our measurement [31].

The MC and data samples are subjected to a preselection requiring: (a) the presence of a converted photon whose reconstructed conversion point ($\mathbf{X}$, $\mathbf{Y}$, $\mathbf{Z}$) be within the fiducial volume, $\mathbf{|X, (Y-5)| \leq 130}$ cm and $\mathbf{Z_{Min} \leq Z \leq 405}$ cm where $\mathbf{Z_{Min}}$ is 5 and 35 cm for the two configurations of the detector composing more than 95% of the NOMAD data; (b) no reconstructed muon ($\boldsymbol{\mu}$ID-veto) and a single photon-induced $\mathbf{V^0}$; (c) the $\mathbf{X}$ and $\mathbf{Y}$ coordinate of the $\boldsymbol{\gamma}$-vector when extrapolated back to the upstream most DC at $\mathbf{Z_{Min}}$ be within the transverse fiducial volume, $\mathbf{|X, Y-5|_{PROJ} \leq 130cm}$, largely eliminating $\boldsymbol{\gamma}$'s that enter from the sides; and (d) the energy of the $\boldsymbol{e^-e^+}$ pair be $\boldsymbol{\geq 1.5}$ GeV which reduces the NC-DIS and OBG background while having a small effect on the Coh$\boldsymbol{\pi^0}$ sample which also serves as a guide for the single $\boldsymbol{\gamma}$ signal. The preselection reduces the NC-DIS and data samples by more than a factor of one hundred. It is noteworthy that only a small fraction of the NC-Res pass the selection since most of the photons, coming from $\boldsymbol{\pi^0}$ emitted at large angles, either fail to trigger the apparatus or have energies below $\mathbf{1.5}$ GeV. Given the paucity of the NC-Resonance events, it has been added to the NC-DIS sample. Finally a negligible fraction of $\boldsymbol{\nu_\mu}$-CC ($\mathbf{< 10^{-5}}$) pass the selection; consequently the CC sample has been ignored in this analysis. The preselection is presented in Table 1.

The final event selection follows the preselection with more stringent requirements. The vertex coordinates of $\mathbf{V^0}$ are required to be within $\mathbf{|X, (Y-5)| \leq 120}$ cm and $\mathbf{Z_{Min} \leq Z \leq 405}$ cm. Two additional cuts (Clean-$\mathbf{V^0}$) are imposed to reduce outside background by requiring that there be no tracks upstream of the photon conversion and that there be no hits associ-

Cut	Coh$\boldsymbol{\pi^0}$ -RS	NC-DIS $\oplus$ Resonance
Start	516	1915
Tighter Fid-Cuts	483	1775
$\boldsymbol{M_{ee} \leq 50}$ MeV & Clean-$\mathbf{V^0}$	386	400

Table 2
Final selection of single $\boldsymbol{\gamma}$ Events in the MC Samples: The MC samples have been normalized as presented in Section 4.

ated with the tracks composing the converted- $\boldsymbol{\gamma}$ in the most upstream DC. Finally, the $\boldsymbol{M_{ee}}$ cut is tightened to $\leq$ **50** MeV which increases the photon conversion purity to $\geq$ **98%** while reducing the efficiency to 93%. Table 2 summarizes the selection of events in the MC samples. The preselected data are subjected to identical cuts. Distributions of the X, Y, and Z coordinates of the 1$\boldsymbol{\gamma}$ vertex in Data and the corresponding MC prediction, composed of Coh$\boldsymbol{\pi^0}$ OBG, NC-DIS, agree. Only the control sample with $\mathbf{PAN < 0.9}$ is examined to check and constrain the background prediction. The calibration of the three backgrounds is presented next.

5 Constraining the Backgrounds and the PAN < 0.9 Sample

The prediction of the backgrounds to the single $\boldsymbol{\gamma}$ sample is data driven. The estimation of the Coh$\boldsymbol{\pi^0}$ induced 1$\boldsymbol{\gamma}$ needs to be based on the observed 2$\mathbf{V^0}$ sample where both photons convert in the DC. Furthermore, Monte Carlo simulations can neither reliably provide the OBG nor the NC-DIS contribution to the 1$\boldsymbol{\gamma}$ samle. These backgrounds need to be determined using data themselves.

First, we present the calibration of the Coh$\boldsymbol{\pi^0}$ contribution to the 1$\boldsymbol{\gamma}$ sample because it is the simplest. The analysis of the 2$\mathbf{V^0}$ sample, where two photons and nothing else is observed, provides a measurement of the Coh$\boldsymbol{\pi^0}$ process. It yields a rate with respect to the inclusive $\boldsymbol{\nu_\mu}$-CC, $[\mathbf{3.21 \pm 0.46}(\boldsymbol{stat \oplus syst})] \times \mathbf{10^{-3}}$ [31]. The measured kinematic distributions of the 2$\boldsymbol{\gamma}$ data are consistent with the RS-Coh$\boldsymbol{\pi^0}$ model. Consequently we use the simulated RS-Coh$\boldsymbol{\pi^0}$ events, normalize it to the measured cross-section, subject these to the 1$\boldsymbol{\gamma}$ analysis, and obtain the Coh$\boldsymbol{\pi^0}$ contribution to the 1$\boldsymbol{\gamma}$ sample. The analysis yields a normalized prediction of Coh$\boldsymbol{\pi^0}$ -induced 1$\boldsymbol{\gamma}$ with a 14.5% precision, shown in Table 4.

Next, we present the calibration of the OBG contribution to the 1$\boldsymbol{\gamma}$ sample. This, too, is accomplished using the 2$\mathbf{V^0}$ sample as in [31]. The two reconstructed photon momentum vectors enable one to determine the $\boldsymbol{\nu}$-interaction vertex by extrapolating the vectors upstream and finding the coordinates of

	DCA-Z≥Zmin	DCA-Z<Zmin
2γ Data	381	169
2γ OBG-Data	451	927

Table 3
Events passing and failing the Z-cut in 2γ samples in Data and OBG-Data

their distance of closest approach (DCA). The procedure defines the DCA-vertex with coordinates denoted as DCA-X, DCA-Y, and DCA-Z. The DCA-vertex resolution is well understood. Among the 2γ sample 169 events, out of 550 events (see Table 3), have a DCA vertex of origin upstream of the $\mathbf{Z_{Min}}$ providing a calibration for the OBG-1γ as follows. A different data sample, OBG-Data, which includes charged tracks, is selected in which the vertex reconstructed using these charged tracks is upstream of the fiducial limit ($\mathbf{Z \leq Z_{Min}}$). In this sample, the charged tracks are ignored and the events subjected to the 2γ analysis (see [31]). This OBG-Data sample with 2γ yields 927 events with $\mathbf{DCA\text{-}Z \leq Z_{Min}}$ and 451 events with $\mathbf{DCA\text{-}Z > Z_{Min}}$ as shown in Table 3. The number of 2γ events with $\mathbf{DCA\text{-}Z > Z_{Min}}$, originating from events occurring at $\mathbf{Z \leq Z_{Min}}$ but producing no visible tracks, is then calculated as $\mathbf{(451/927) \times 169 = 82.2 \pm 6.1}$. This constitutes the OBG background to the 2γ sample. The so normalized OBG sample is then subjected to the 1γ analysis yielding a calibrated OBG prediction, with a 7.7% error (driven by the statistics of 169 events), shown in Table 4.

Finally, we present the calibration of the NC-DIS contribution to the 1γ sample using the control region $\mathbf{PAN < 0.9}$ dominated by events containing a photon-conversion accompanied by a neutral energy cluster in the ECAL. Figure 2 shows the observed **PAN** distribution for the full 1γ sample although the signal region $\mathbf{PAN \geq 0.9}$ is not looked at till all backgrounds are finalized. The figure evinces agreement between data and the prediction for $\mathbf{PAN < 0.9}$. Furthermore, the observed kinematic variables associated with the neutral cluster in ECAL are found to be consistent with the prediction. The observed momentum distribution of the photon is consistent with the prediction as evidenced by Figure 3. Lastly, Figure 4 shows that the measured $\boldsymbol{\zeta_\gamma}$ distribution agrees with the MC prediction. Because the $\boldsymbol{\pi^0}$ -induced photons in NC-DIS will have a broader $\boldsymbol{\zeta_\gamma}$ than those in Coh$\boldsymbol{\pi^0}$, we use $\boldsymbol{\zeta_\gamma > 0.05}$ to normalize the NC-DIS. The NC-DIS normalization factor is $\mathbf{1.13 \pm 0.14}$. (This normalization factor has been applied to the NC-DIS in the figures.) The logic behind using this control sample to constrain the background in the signal region is that 1γ events come from $\boldsymbol{\pi^0}$-dominated neutral current events where one of the photons evades detection. One concern, however, is that of a possible systematic bias when using the $\mathbf{PAN < 0.9}$, a region where both photons are reconstructed in DC and ECAL, i.e. the two photons are emitted in the forward direction, to predict the NC-DIS in the $\mathbf{PAN \geq 0.9}$ where the second photon misses the ECAL. To check this concern, ordinary

NC events, where charged tracks define the event, and, thereby, relieving the forward bias in the 1γ reconstruction due to the trigger requirement, are selected in data and MC. A single 1γ is selected downstream of the event. The charged tracks are ignored, the 1γ is subjected to the current analysis. The Data/MC ratio is examined in $\boldsymbol{E_\gamma}$ and $\boldsymbol{\zeta_\gamma}$ variables. The check reveals that the shapes of these variables in MC are consistent with those of data: the ratio is unity within $\pm\mathbf{5\%}$ in the kinematic range, well covered by the 12% error ascribed to the NC-DIS. Table 4 presents the NC-DIS contribution to the 1γ sample.

To sum up, we have a calibrated prediction of Coh$\boldsymbol{\pi^0}$, OBG, and NC-DIS contributions to the 1γ sample. Table 4 lists the corresponding errors, all statistical in nature, as determined by the respective data control samples. Additionally, we estimate the error in the 1γ reconstruction to be $\leq \mathbf{2.5\%}$, which has a negligible effect on this analysis. As a final check, we reproduced the results presented in the [21]. This exercise illustrates that the current analysis is two orders of magnitude less stringent than that in [21] which was focussed on the search for a heavy neutrino coupling to $\boldsymbol{\nu_\tau}$.

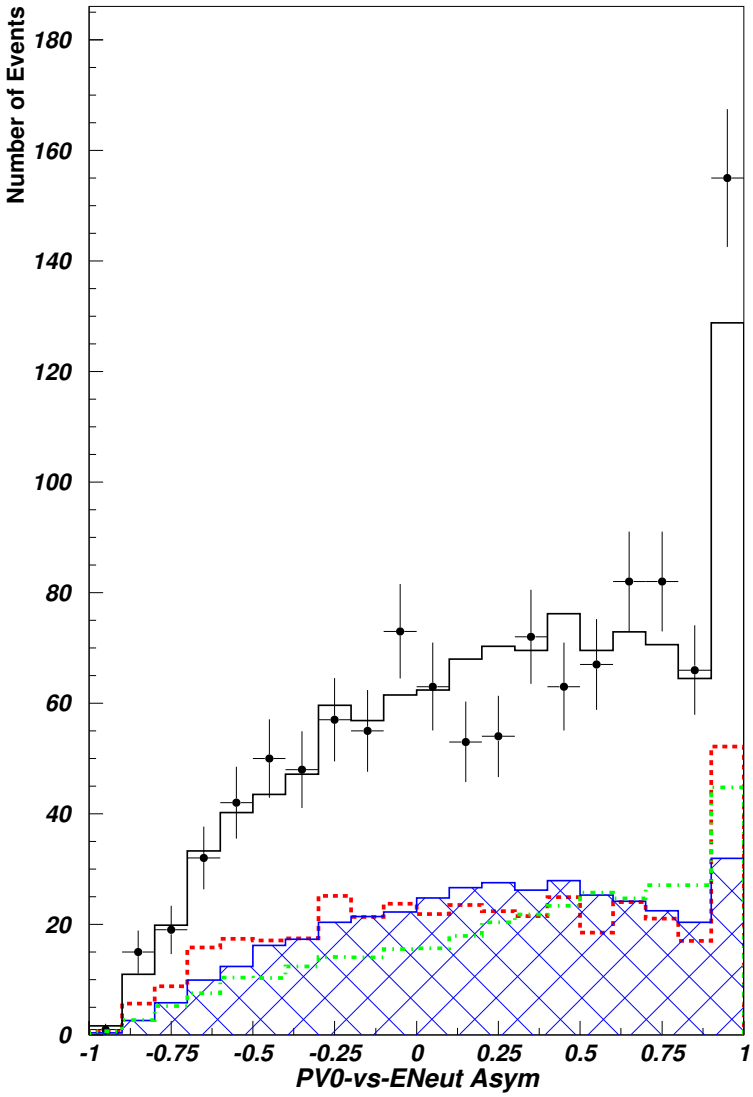

Fig. 2. Comparison of **PAN** , the energy asymmetry between the 1γ -momentum and the neutral energy in the ECAL, between Data (Symbol) and prediction: Coh$\boldsymbol{\pi^0}$ (Blue-hatched), OBG (Green-dash-dot), NC-DIS (Red-dash), and total (Black-histogram). The signal region, **PAN** $\geq$ **0.9**, is not looked at till the analysis is complete.

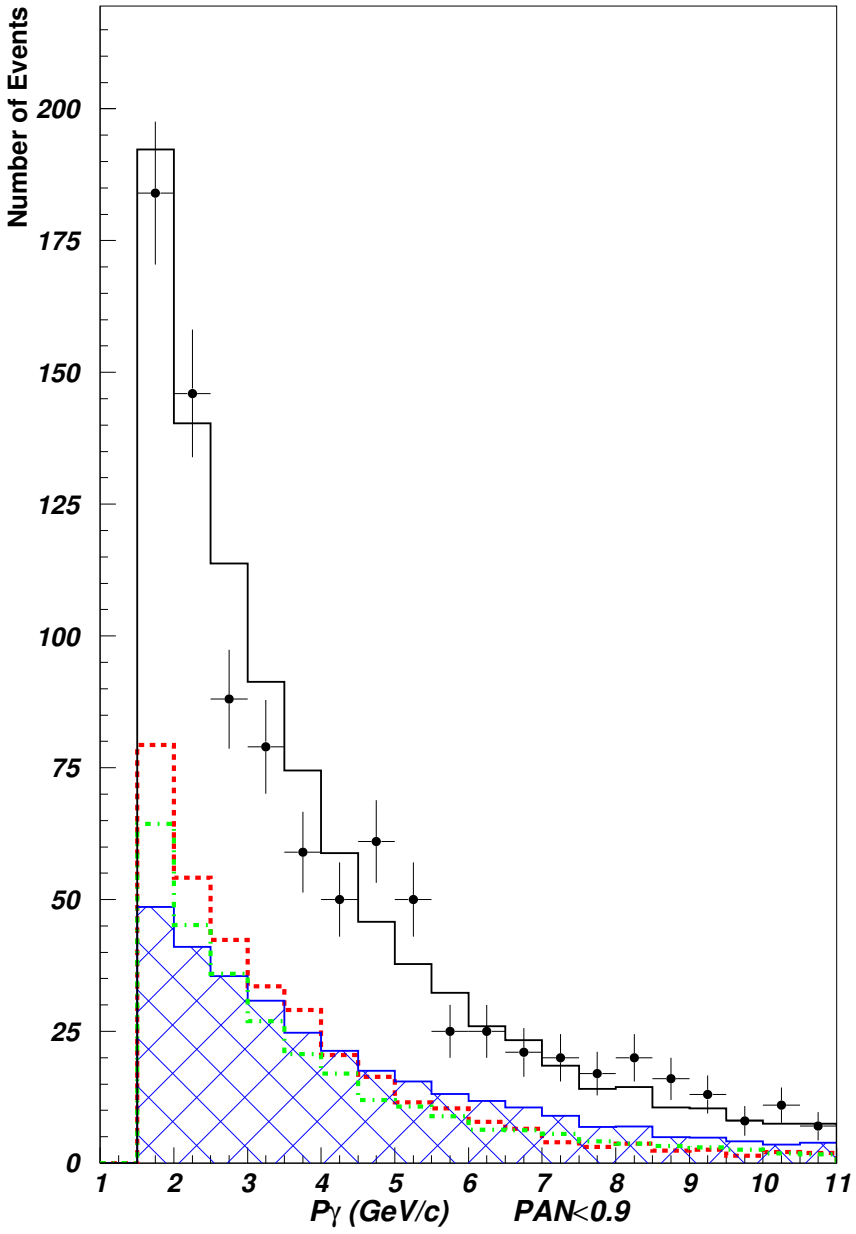

Fig. 3. Comparison of P_γ between data and MC in **PAN < 0.9** region.

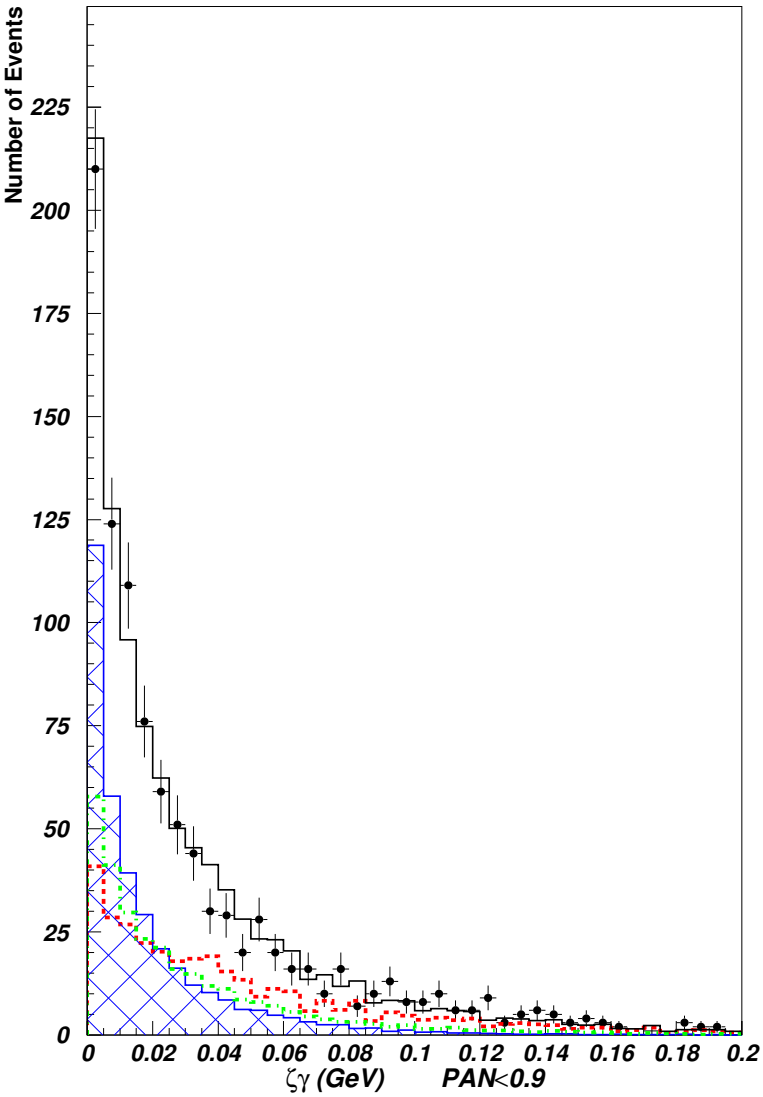

Fig. 4. Comparison of ζ_γ distribution of the 1γ sample with $\mathbf{PAN < 0.9}$ in data and MC. The $\zeta_\gamma > \mathbf{0.05}$ region is used to normalize the NC-DIS.

6 Results

Figure 1 shows a representative event in the signal region, $\mathbf{PAN \geq 0.9}$. The first signal-box, **Box1**, with $\mathbf{PAN \geq 0.9}$, yields 155 observed events with a predicted background $\mathbf{129.2 \pm 8.5 \pm 3.3}$ events yielding an excess of $\mathbf{25.8 \pm 15.5}$ events. Figure 5 and Figure 6 present the $\boldsymbol{P}_\gamma$ and $\boldsymbol{\zeta}_\gamma$ comparison between data and MC. Absence of significant excess leads us to interpret this as null evidence for excess of single photon events. Assuming the error on the background-prediction to be Gaussian, we derive an upper limit of $< \mathbf{51}$ events at 90% CL in **Box1**.

The second signal-box, **Box2**, with $\mathbf{PAN \geq 0.9}$ and $\boldsymbol{\zeta}_\gamma \leq \mathbf{0.05}$, yields 78 ob-

Cut	Cohπ^0 -RS	NC-DIS$\oplus$Res	OBG	Total	Data
$\mathbf{V^0}$ sample	385.9	400.1	341.3	1127.3	1149
MC Error	14.5%	12.0%	7.7%		
Background					
PAN < 0.9	353.9	347.7	296.5	998.1 $\pm$69.9$\pm$25.0	994
Signal					
PAN ≥ 0.9	32.0	52.4	44.8	129.2$\pm$8.5$\pm$3.3	155
PAN $\geq 0.9 \oplus \zeta_\gamma \leq 0.05$	22.8	22.6	31.2	76.6$\pm$4.9$\pm$1.9	78

Table 4
The 1γ Sample: Presented are the normalized Cohπ^0 , NC-DIS, and OBG predictions for the 1γ sample. The MC errors of the three components are all statistical in nature, as determined by the respective control samples. The systematic error due the $\mathbf{V^0}$ -reconstruction is shown under the 'Total' column. Data are shown in the last column.

served events with a predicted background $\mathbf{76.6 \pm 4.9 \pm 1.9}$ events yielding an excess of $\mathbf{1.4 \pm 10.3}$ events. Events in the **Box2** exhibit kinematic characteristics consistent with the background prediction. The vertex-distributions of the 1γ events in the signal-region are in agreement with the MC prediction; as are, within errors, the $\boldsymbol{P_\gamma}$ and $\boldsymbol{\zeta_\gamma}$ distributions, shown in Figure 7 and Figure 6. In addition, the observed collinearity ($\boldsymbol{\mathcal{C}}$) of the photon matches that of the prediction, see Figure 8. Assuming the error to be Gaussian, we derive an upper limit of $\mathbf{< 18}$ events at 90% CL. Table 4 presents the final enumeration.

The only remaining task is to set an upper limit on the rate of single $\boldsymbol{\gamma}$ events. To determine the signal efficiency, we assume that the 'signal' photon has kinematics similar to that of one of the photons from the Coh$\boldsymbol{\pi^0}$ interaction (the other photon is removed from the simulation). Using the RS Coh$\boldsymbol{\pi^0}$ -model, the signal efficiency for **Box1**, $\mathbf{PAN \geq 0.9}$, is 8.8%. The efficiency for **Box2**, $\mathbf{PAN \geq 0.9}$ and $\boldsymbol{\zeta \leq 0.05}$, is 8.0%. The number of fully corrected $\boldsymbol{\nu_\mu}$-CC in the same fiducial volume is measured to be $\mathbf{1.44 \times 10^6}$. We obtain the following upper limits on the rate of single photon events in $\boldsymbol{\nu}$-interactions:

$$\frac{\boldsymbol{\sigma(\mathrm{Single} - \gamma)}}{\boldsymbol{\sigma(\nu_\mu \mathcal{A} \to \mu^- X)}} < \mathbf{4.0 \times 10^{-4} (90\%CL)} \tag{1}$$

$$\frac{\boldsymbol{\sigma(\mathrm{Single, Forward} - \gamma)}}{\boldsymbol{\sigma(\nu_\mu \mathcal{A} \to \mu^- X)}} < \mathbf{1.6 \times 10^{-4} (90\%CL)} \tag{2}$$

In summary, we have presented a search for single photon events in interactions of neutrinos with average energy $\boldsymbol{E_\nu \simeq 25}$ GeV. All relevant backgrounds are constrained using data control samples. No significant excess is seen. Assuming that the hypothetical signal has kinematics similar to those of a photon from the Coh$\boldsymbol{\pi^0}$ interaction, the analysis imposes an upper limit on the rate of excess of single photon events of $\boldsymbol{< 4.0 \times 10^{-4}}$ per $\boldsymbol{\nu_\mu}$-CC at 90% CL; with an additional soft collinearity cut (permitting 90% of $\boldsymbol{\gamma}$ from Coh$\boldsymbol{\pi^0}$) the limit is $\boldsymbol{< 1.6 \times 10^{-4}}$ per $\boldsymbol{\nu_\mu}$-CC at 90% CL. Following the report on superluminal neutrinos by the OPERA collaboration [32], we are conducting a specialized search for very forward $\boldsymbol{e^- e^+}$ pairs.

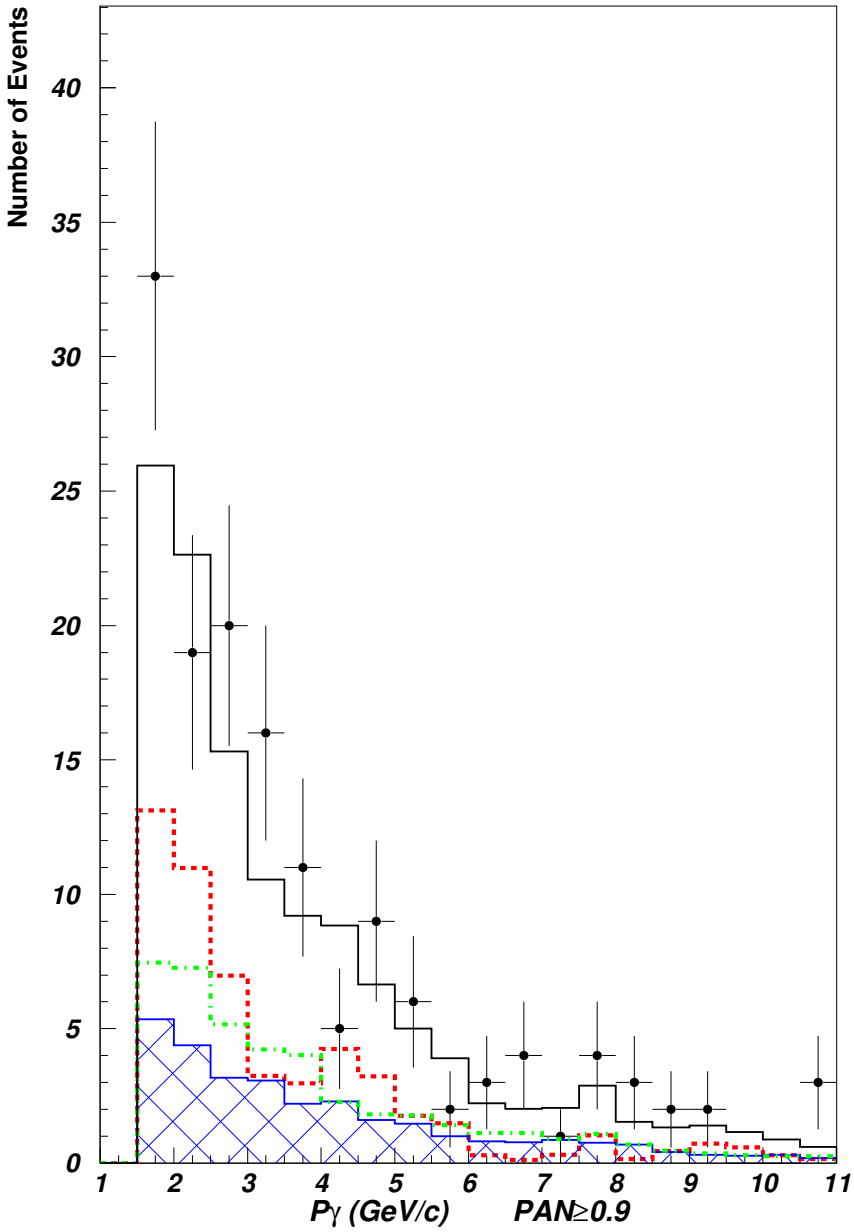

Fig. 5. Comparison of P_γ between data and MC in **Box1**, **PAN** $\geq$ **0.9** region.

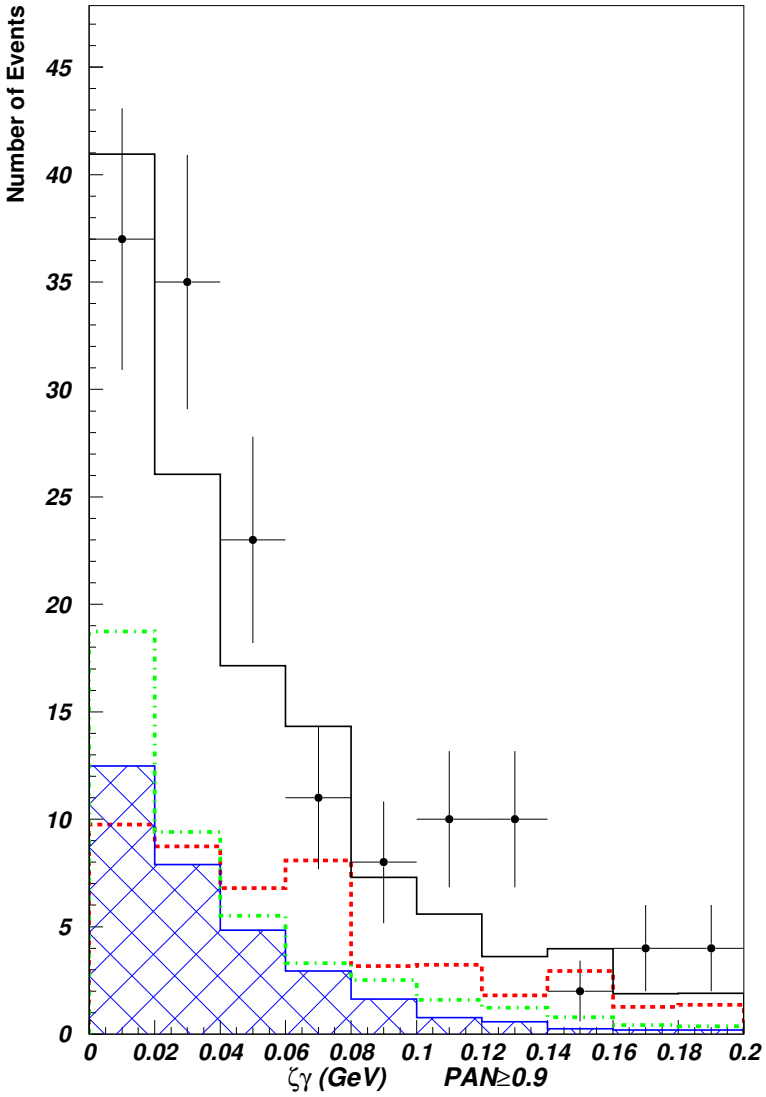

Fig. 6. Comparison of ζ_γ distribution between data and MC in **Box1**, **PAN** $\geq$ **0.9** region.

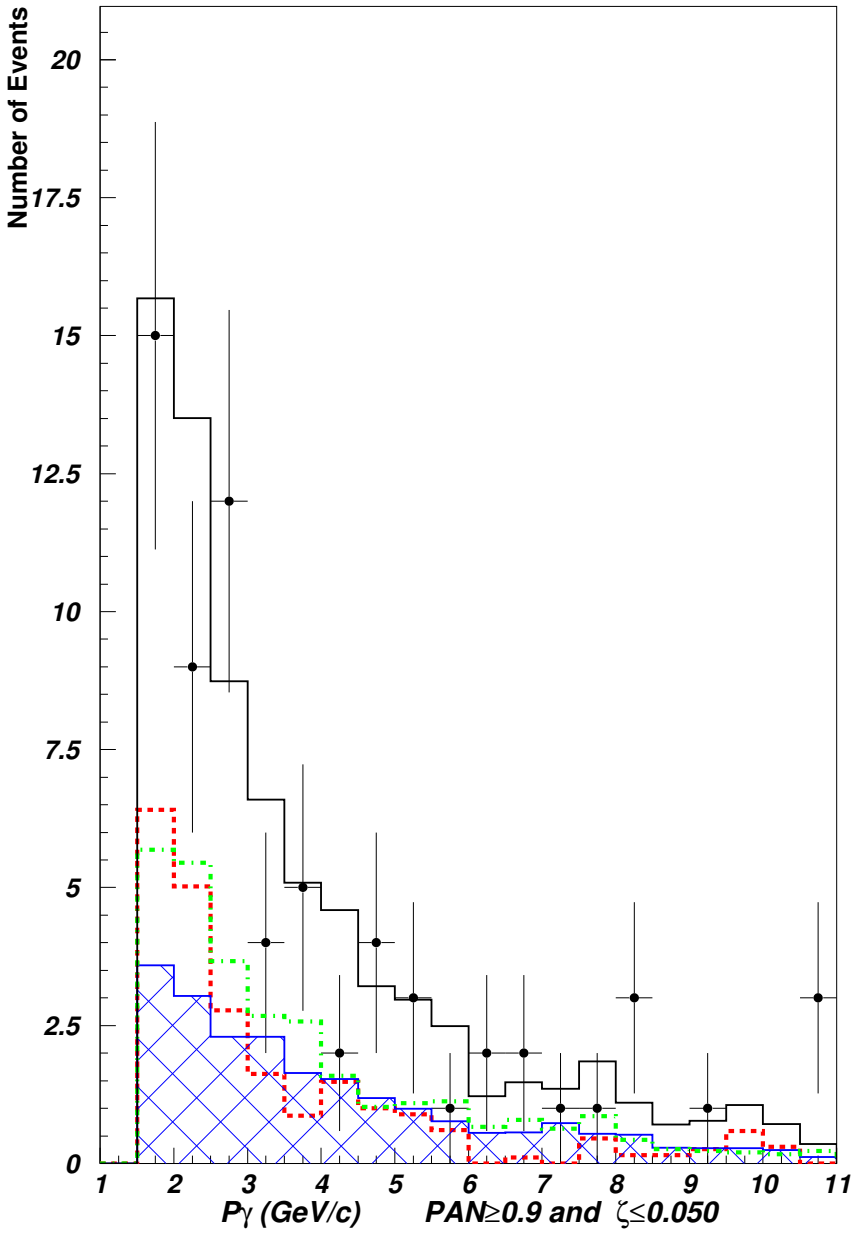

Fig. 7. The Momentum of 1γ in **Box2**: The observed distribution is consistent with the MC-prediction.

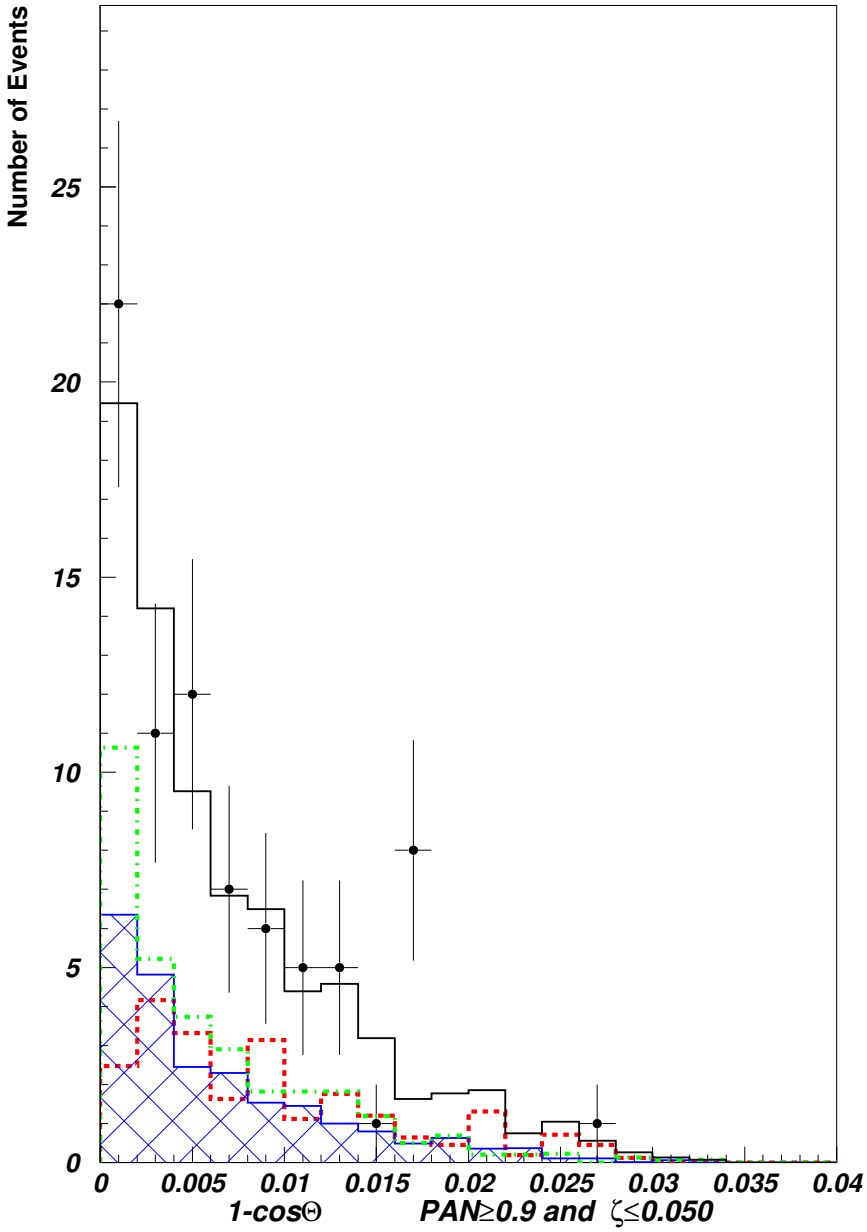

Fig. 8. Consistent collinearity of 1γ in data and MC in the **Box2**.

Acknowledgments

We extend our grateful appreciations to the CERN SPS staff for the magnificent performance of the neutrino beam. We (CTK and SRM) warmly thank Bill Louis, Richard Hill, Chris Hill, James Jenkins and Terry Goldman for many stimulating discussions and insights. The experiment was supported by the following agencies: ARC and DIISR of Australia; IN2P3 and CEA of France, BMBF of Germany, INFN of Italy, JINR and INR of Russia, FNSRS of Switzerland, DOE, NSF, Sloan, and Cottrell Foundations of USA, and VP

Research Office of the University of South Carolina.

References

[1] A. A. Aguilar-Arevalo *et al.* [MiniBooNE Collaboration], Phys. Rev. Lett. **102**, 101802 (2009) [arXiv:0812.2243 [hep-ex]].

[2] A. A. Aguilar-Arevalo *et al.* [MiniBooNE Collaboration], Phys. Rev. Lett. **98**, 231801 (2007) [arXiv:0704.1500 [hep-ex]].

[3] A. A. Aguilar-Arevalo *et al.* [MiniBooNE Collaboration], Phys. Rev. Lett. **103**, 111801 (2009)

[4] Z. Djurcic for the MiniBooNE Collaboration, at NuFact 2011, Geneva, Switzerland.

[5] A. Bodek, arXiv:0709.4004 [hep-ex].

[6] A. A. Aguilar-Arevalo *et al.* [MiniBooNE Collaboration], arXiv:0710.3897 [hep-ex].

[7] J. A. Harvey, C. T. Hill and R. J. Hill, Phys. Rev. Lett. **99**, 261601 (2007) [arXiv:0708.1281 [hep-ph]].

[8] J. A. Harvey, C. T. Hill and R. J. Hill, Phys. Rev. D **77**, 085017 (2008) [arXiv:0712.1230 [hep-th]].

[9] J. Jenkins and T. Goldman, Phys. Rev. D **80**, 053005 (2009) [arXiv:0906.0984 [hep-ph]].

[10] R. J. Hill, Phys. Rev. D **81**, 013008 (2010) [arXiv:0905.0291 [hep-ph]].

[11] S. N. Gninenko, Phys. Rev. Lett. **103**, 241802 (2009) [arXiv:0902.3802 [hep-ph]].

[12] S. N. Gninenko, Phys. Rev. D **83**, 015015 (2011) [arXiv:1009.5536 [hep-ph]].

[13] M. Maltoni and T. Schwetz, Phys. Rev. D **76**, 093005 (2007) [arXiv:0705.0107 [hep-ph]].

[14] T. Goldman, G.J. Stephenson Jr., B. H. J. McKellar, Phys. Rev. D75 (2007) 091301.

[15] H. Pas, S. Pakvasa and T. J. Weiler, Phys. Rev. D **72**, 095017 (2005) [arXiv:hep-ph/0504096].

[16] C. Giunti and M. Laveder, Phys. Rev. D **83**, 053006 (2011) [arXiv:1012.0267 [hep-ph]]; arXiv:1107.1452 [hep-ph]; arXiv:1109.4033 [hep-ph].

[17] T. Katori, V. A. Kostelecky and R. Tayloe, Phys. Rev. D **74**, 105009 (2006) [arXiv:hep-ph/0606154].

[18] V. Barger, D. Marfatia and K. Whisnant, Phys. Lett. B **576**, 303 (2003) [arXiv:hep-ph/0308299].

[19] A. E. Nelson and J. Walsh, Phys. Rev. D **77**, 033001 (2008) [arXiv:0711.1363 [hep-ph]].

[20] Y. Farzan, T. Schwetz and A. Y. Smirnov, JHEP **0807**, 067 (2008) [arXiv:0805.2098 [hep-ph]].

[21] P. Astier *et al.* [NOMAD collaboration], Phys. Lett. **B506**, 27-38 (2001). [hep-ex/0101041].

[22] P. Astier *et al.* [NOMAD collaboration], NIM A515, 800-828 (2003)

[23] G. Ambrosini *et al.* [SPY Collaboration], Phys. Lett. B **420**, 225 (1998).

[24] G. Ambrosini *et al.* [SPY Collaboration], Phys. Lett. B **425**, 208 (1998).

[25] G. Ambrosini *et al.* [SPY Collaboration], Eur. Phys. J., C 10 (1999) 605-627

[26] H.W. Atherton *et al.*, CERN Yellow Report 80-07, 1980.

[27] J. Altegoer *et al.* [NOMAD collaboration], NIM A404, 96-128 (1998)

[28] P. Astier *et al.* [NOMAD collaboration], Nucl. Phys. B611, 3-39 (2001)

[29] Q. Wu *et al.* [NOMAD Collaboration], Phys. Lett. B **660**, 19 (2008) [arXiv:0711.1183 [hep-ex]].

[30] D. Rein and L. M. Sehgal, Nucl. Phys. B **223**, 29 (1983).

[31] C. T. Kullenberg *et al.* [NOMAD Collaboration], Phys. Lett. B **682**, 177 (2009) [arXiv:0910.0062 [hep-ex]].

[32] T. Adam *et al.* [OPERA Collaboration], arXiv:1109.4897 [hep-ex].